Nonlinear Electrohydrodynamic Stability of Two Superposed Bounded Fluids in the Presence of Interfacial Surface Charges

M. F. El-Sayed and D. K. Callebaut

Physics Department (UIA), University of Antwerp, B-2610 Wilrijk, Belgium

Z. Naturforsch. **53a**, 217–232 (1998); received January 23, 1998

The method of multiple scales is used to analyse the nonlinear propagation of waves on the interface between two superposed dielectric fluids with uniform depths in the presence of a normal electric field, taking into account the interfacial surface charges. The evolution of the amplitude for travelling waves is governed by a nonlinear Schrödinger equation which gives the criterion for modulational instability. Numerical results are given in graphical form, and some limiting cases are recovered. Three cases, in the pure hydrodynamical case, depending on whether the depth of the lower fluid is equal to or greater than or smaller than the one of the upper fluid are considered, and the effect of the electric field on the stability regions is determined. It is found that the effect of the electric field is the same in all the cases for small values of the field, and there is a value of the electric field after which the effect differs from case to case. It is also found that the effect of the electric field is stronger in the case where the depth of the lower fluid is larger than the one of the upper fluid. On the other hand, the evolution of the amplitude for standing waves near the cut-off wavenumber is governed by another type of nonlinear Schrödinger equation with the roles of time and space are interchanged. This equation makes it possible to determine the nonlinear dispersion relation, and the nonlinear effect on the cut-off wavenumber.

Key words: Hydrodynamic Stability; Electrohydrodynamics; Nonlinearity; Interfacial Instability; Dielectric Fluids; Surface Charges.

1. Introduction

The two-dimensional evolution of a nonlinear wave packet propagating on deep water has been investigated by Lighthill [1], Whitham [2], and Yuen and Lake [3], using the method of averaged Lagrangian. Also Chu and Mei [4], Hasimoto and Ono [5] used the multiple scales method to study the same problem. All the above authors derived two-dimensional nonlinear Schrödinger equation describing the modulation of the wave amplitude. Zakharov [6] showed that this equation provides an elegant approach to examine the modulational instability of finite amplitude waves. It was shown by Yuen and Lake [3] that the nonlinear Schrödinger equation can be derived by the averaged Lagrangian method when the spatial variations in the amplitude are included in the dispersion relation. Moreover, they demonstrated that the two-dimensional nonlinear Schrödinger equation provides a quantitative satisfactory description of the long-time evolution of weakly nonlinear wave packets.

Reprint requests to Dr. M. F. El-Sayed:
Department of Mathematics, Faculty of Education,
Ain Shams University, Roxy, Cairo, Egypt.

The nonlinear modulation of waves propagating along the interface between two liquid layers has been investigated by Qi-su [7] and Tanaka [8]. By using the method of multiple scales, the evolution equation of a wave packet of the wave train has been found. Then they discussed the stability of a wave train with infinitesimal perturbation in the direction of propagation of the wave train and obtained the stability criterion. But their theory can not be used to discuss the instability when transverse perturbation occurs. For recent works concerning the instability of capillary-gravity waves, see the work of Chhabra and Khosla [9], Christodulides and Dias [10], Collin *et al.* [11], Jones [12], Dolai [13], Qingpu [14], Lee [15], and Kato *et al.* [16].

On the other hand, electrohydrodynamics is the field of the mechanics of continua that studies the motion of media interacting with the electric field. Such an interaction takes place as a result of action of the Coulomb force upon a medium, or as a result of work of the electric field in flowing of currents. The motion of a medium gives rise to re-distribution of a volume charge, which results in changing the electric field and, hence, the force acting on a medium. In the majority of problems under consideration, electric fields or electric charges are specified by external sources. Such a situation takes place

0932-0784 / 98 / 0500-0217 $ 06.00 © – Verlag der Zeitschrift für Naturforschung, D-72027 Tübingen

during operation of electrohydrodynamic generators, pumps, separators, filters, and other devices. This subject is treated in a vast literature. The last studied is the class of electrohydrodynamic problems in which the electric field or electric charges arise as a result of a contact between media of different nature: liquid-solid body, liquid-gas or two different liquids (see [17]–[22]).

The effect of the electric field on the motion of fluids has been studied by a number of scientists since the pioneering work of Rayleigh [23], Stokes [24], and Melcher [25]. Michael [26] investigated the stability of an incompressible, inviscid, perfectly conducting fluid layer in the presence of electrostatic forces, and he found that these forces can have a destabilising effect on the fluid motions. Shivamoggi [27] has also examined the stability of such a problem in the neighbourhood of the linear cut-off wavenumber. Kant *et al.* [28] investigated the stability of weakly nonlinear waves on the surface of a perfectly conducting fluid layer in the presence of an applied electric field by using the derivative expansion method. The nonlinear electrohydrodynamic Rayleigh-Taylor instability was investigated by Mohamed and Elshehawey [29]. They obtained two nonlinear Schrödinger equations by means of which one can deduce the cut-off wavenumber and analyze the stability of the system. Quite recently, Elshehawey [30] investigated the same problem of Rayleigh-Taylor instability for a normal periodic electric field and the intervals of stability conditions. For recent works concerning the linear and nonlinear electrohydrodynamic instability at the interface between two fluids, see [31]–[34], and for an excellent review of the subject, see the recent review of Saville [35].

In this paper, the interfacial stability of two superposed dielectric fluids of finite depths is investigated with the effect of normal electric fields in the presence of surface charges on the surface of separation between the two fluids. The stability here is discussed in detail for the cases of travelling and standing waves, and the results of Hasimoto and Ono [5], Qi-su [7], and Mohamed and Elshehawey [29] are extended.

2. Formulation of the Problem

We consider the two-dimensional wave motion on the interface $y = 0$ between the two superposed dielectric fluids with uniform depths, the upper fluid having the density $\rho^{(2)}$, dielectric constant $\varepsilon^{(2)}$ and being bounded by the conducting plane $y = b_0$ which is raised to the potential V_0 whereas the lower fluid with density $\rho^{(1)}$, dielectric constant $\varepsilon^{(1)}$ is bounded from below by an earthed conducting plane $y = -a_0$. As a result of the potential difference between the planes, both fluids are subjected to a constant electric field normal to the interface $E_0^{(2)}$ and $E_0^{(1)}$, where the superscripts 1 and 2 refer to the lower and upper fluids, respectively.

If the two fluids are assumed to be inviscid and incompressible, and the fluid motion being irrotational, then there exist velocity potentials $\phi^{(j)}(x, y, t)$ within the two regions such that $\mathbf{v}^{(j)} = \nabla\phi^{(j)}$. Since the system is stressed by a normal electric field, we shall assume that it allows for the presence of surface charges at the interface such that $\varepsilon^{(1)}E_0^{(1)} \neq \varepsilon^{(2)}E_0^{(2)}$.

We shall assume that the quasi-static approximation is valid and the electric field $\boldsymbol{E}$ is irrotational. The electric potentials $\psi^{(j)}$ are defined such that

$$\boldsymbol{E}^{(j)} = -E_0^{(j)}\boldsymbol{e}_y - \nabla\psi^{(j)},$$

$$E_0^{(j)} = \frac{V_0\varepsilon^{(j\pm1)}}{(\varepsilon^{(2)}b_0 + \varepsilon^{(1)}a_0)}, \tag{1}$$

where $\boldsymbol{e}_y$ is the unit vector in the y-direction.

The basic equations relevant to our problem, are

$$\phi_{xx}^{(j)} + \phi_{yy}^{(j)} = 0 \quad \text{and} \quad \psi_{xx}^{(j)} + \psi_{yy}^{(j)} = 0,$$

$$j = 1, 2. \tag{2}$$

where $j = 1, 2$ represet the regions $-h < y < \eta(x, t)$ and $\eta(x, t) < y < b_0$, respectively, $y = \eta(x, t)$ is the elevation of the interface measured from the unperturbed level, and t denotes the time.

The various physical quantities are normalized with respect to a characteristic length $l_c = (T/\rho^{(1)}g)^{1/2}$ and a characteristic time $t_c = (l_c/g)^{1/2}$ and the characteristic potential functions $\phi_c = (gl^3)^{1/2}$, $\psi_c = (\rho^{(1)}gl_c^3)^{1/2}$, where g is the acceleration due to gravity acting in the negative y-direction and T is the surface tension. Hence we have $l = l_c l'$, $t = t_c t'$, $\phi^{(j)} = \phi_c\phi'^{(j)}$ and $\psi^{(j)} = \psi_c\psi'^{(j)}$, where l', t', $\phi'^{(j)}$ and $\psi'^{(j)}$ are dimensionless; next we drop the primes for simplicity.

The boundary conditions at the interface $y = \eta(x, t)$ are [36]

$$\eta_t - \phi_y^{(j)} + \eta_x\phi_x^{(j)} = 0, \quad j = 1, 2, \tag{3}$$

$$\eta_x\langle\langle\psi_y\rangle\rangle + \langle\langle\psi_x\rangle\rangle = \eta_x\langle\langle E_0\rangle\rangle, \tag{4}$$

$$\eta_x\langle\langle\varepsilon\psi_x\rangle\rangle - \langle\langle\varepsilon\psi_y\rangle\rangle = 0, \tag{5}$$

$$\phi_t^{(1)} - \rho\phi_t^{(2)} + (1-\rho)\eta + \frac{1}{2}\left(\phi_x^{(1)^2} - \rho\phi_x^{(2)^2}\right) + \frac{1}{2}\left(\phi_y^{(1)^2} - \rho\phi_y^{(2)^2}\right) =$$

$$= \eta_{xx}(1+\eta_x^2)^{-\frac{3}{2}} - \frac{1}{2}\left\langle\!\left\langle \varepsilon\psi_x^2 \right\rangle\!\right\rangle + \frac{1}{2}\left\langle\!\left\langle \varepsilon\psi_y^2 \right\rangle\!\right\rangle - \left\langle\!\left\langle \varepsilon E_0\psi_y \right\rangle\!\right\rangle + 2\eta_x\left\langle\!\left\langle \varepsilon E_0\psi_x \right\rangle\!\right\rangle - 2\eta_x\left\langle\!\left\langle \varepsilon\psi_x\psi_y \right\rangle\!\right\rangle \tag{6}$$

$$- \eta_x^2\left\langle\!\left\langle \varepsilon E_0^2 \right\rangle\!\right\rangle + 2\eta_x^2\left\langle\!\left\langle \varepsilon E_0\psi_y \right\rangle\!\right\rangle + \text{higher order terms},$$

where $\rho = \rho^{(2)}/\rho^{(1)}$, and $\langle\!\langle\cdot\rangle\!\rangle$ represents the jump across the interface.

The solutions $\phi^{(j)}$, $\psi^{(j)}$ of (2) must satisfy the following conditions at the boundaries $y = -a, b$:

$$\phi_y^{(j)}, \psi_x^{(j)} = 0 \quad \text{on} \quad y = -a, b, \tag{7}$$

where a and b are the dimensionless quantities for the depths.

To investigate the modulation of a weakly nonlinear wave with narrow band width spectrum, we employ the method of multiple scales [37] by introducing the variables $x_n = \tilde{\varepsilon}^n x$ and $t_n = \tilde{\varepsilon}^n t$, $(n = 0, 1, 2, 3)$, and expanding η, $\phi^{(j)}$ and $\psi^{(j)}$, $j = 1, 2$ in the asymptotic series

$$F(x,y,t) = \sum_{n=1}^{3} \tilde{\varepsilon}^n F_n(x_0, x_1, \ldots, x_N, y, t_0, t_1, \ldots t_N) + O(\tilde{\varepsilon}^4), \tag{8}$$

where the small parameter $\tilde{\varepsilon}$ characterizes the steepness ratio of the wave, and the expansion of η according to (9) is independent of y.

Expanding now the boundary conditions (3)–(7) into Maclaurin series expansions around $y = 0$, then substituting (8) into (2) and the boundary conditions (3)–(7), and equating the coefficients of equal powers in $\tilde{\varepsilon}$, we obtain the linear and successive nonlinear partial differential equations for η_n, ϕ_n and $\psi_n^{(1),(2)}$ [36]; they will not be given because they are very lengthy.

3. Linear Theory

We assume that there is no steady flow in the undisturbed state, so that we choose the following quasi-monochromatic wave as the starting solutions to the first order problem

$$\eta_1 = i\sigma_1 A e^{i\theta} + c.c., \tag{9}$$

$$\phi_1^{(1)} = \frac{\omega\cosh(ky + a')}{k\cosh a'} A e^{i\theta} + c.c. + B_1^{(1)}, \tag{10}$$

$$\phi_1^{(2)} = -\frac{\omega\cosh(ky - b')}{k\cosh b'}\frac{\sigma_1}{\sigma_2} A e^{i\theta} + c.c. + B_1^{(2)}, \tag{11}$$

$$\psi_1^{(1)} = iE_0^{(1)}\frac{\sinh(ky + a')}{\cosh a'} A e^{i\theta} + c.c., \tag{12}$$

$$\psi_1^{(2)} = -\frac{iE_0^{(2)}\sigma_1}{\sigma_2}\frac{\sinh(ky - b')}{\cosh b'} A e^{i\theta} + c.c., \tag{13}$$

where $a' = ka$, $b' = kb$, $\sigma_1 = \tanh a'$, $\sigma_2 = \tanh b'$, and $\theta\,(= kx_0 - \omega t_0)$ is the phase of the carrier wave, k and ω being, respectively, the wavenumber and frequency of the centre of the wave packets, and c.c. stands for the complex conjugate of the preceding term (or terms), and i is the imaginary unit. Here, the complex amplitude A and the additional real constants $B_1^{(j)}$ (which represent the arbitrariness associated with the velocity potential) are functions of the slow scales x_1, x_2, t_1, and t_2.

In order that the starting solution should not be trivial, the wavenumber k and the frequency ω must satisfy the dispersion relation

$$\omega^2 = k\left(\frac{1}{\sigma_1} + \frac{\rho}{\sigma_2}\right)^{-1} \cdot \left[1 - \rho + k^2 - k\left(\frac{V_2^2}{\sigma_2} + \frac{V_1^2}{\sigma_1}\right)\right], \tag{14}$$

where

$$V_j^2 = \varepsilon^{(j)} E_0^{(j)^2}, \quad j = 1, 2.$$

The dispersion relation (14) was initially obtained by Melcher [25], Mohamed and Elshehawey [29] (for the case of two-dimensional, semi-infinite fluids), and also by Qi-Su [7] (for the corresponding hydrodynamical case, i.e. when $E_0^{(j)} = 0$ or $\varepsilon^{(1)} = \varepsilon^{(2)}$). The critical wavenumber k_c at which $\omega = 0$ is the linear electrohydrodynamic cut-off wavenumber separating stable from unstable disturbances. For a numerical discussion of the dispersion equation (14), we have a transition curve, namely

$$k^2 - k\left(\frac{V_2^2}{\sigma_2} + \frac{V_1^2}{\sigma_1}\right) + (1 - \rho) = 0. \tag{15}$$

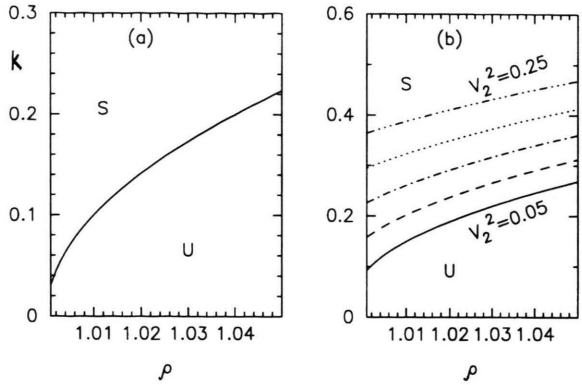

Fig. 1. Stability diagram for the linear case in the k-ρ plane for some values of the electric field variations V_1^2, V_2^2, and the density ratio $\rho > 1$. The curve in Fig. 1 a corresponds to the values $V_1^2 = V_2^2 = 0$. The solid, dashed, dot-dashed, dotted and 3 dot-dashed curves in Fig. 1 b correspond respectively to the values $V_2^2 = 0.05$, 0.1, 0.15, 0.2 and 0.25 where $V_1^2 = 0.009$ and $a' = b' = 0.9$.

From (15) we calculated the values of k corresponding to some different values of V_1^2 and V_2^2 in the cases when $a' = b'$, $a' > b'$ and $a' < b'$, respectively, for values of the density parameter $\rho \geq 1$. We plotted the neutral stability condition (15), separating the stable S and unstable U regions. Figures 1 and 2 are the stability diagrams for the linear case in the $k - \rho$ plane for different values of the electric field variations.

Figure 1 a is drawn for the case of no electric field influence, i.e. $V_1^2 = V_2^2 = 0$ for any depths of the fluids. The resulting curve represent the neutral curve separating the stable and unstable regions. Figure 1 b is drawn for the case of equal depths (i.e. $a' = b' = 0.9$), and the resulting curves correspond to the electric field values $V_2^2 = 0.05$, 0.1, 0.15, 0.2 and 0.25, respectively, with $V_1^2 = 0.009$. It is clear from Fig. 1 a that increasing the electric field values increases the unstable region, i.e. the electric field has a destabilizing effect.

Figure 2 a is drawn for the case when the lower depth is greater than the upper one (i.e. $a' > b'$, where $a' = 0.9$ and $b' = 0.3$), while Fig. 2 b is drawn for the case when the lower depth is less the upper one (i.e. $a' < b'$, where $a' = 0.3$ and $b' = 0.9$). The resulting curves in Fig. 2 correspond to the same values of the electric field mentioned in Figure 1 b. It is clear from Fig. 2 that the normal electric field has usually a destabilizing effect and that the effect is stronger or faster in the case $a' > b'$ than the other cases when $a' < b'$ and $a' = b'$.

Now, to derive the equation for the evolution of travelling waves, we need to proceed to the second order and higher order problems.

4. Second Order Solution

Since our aim is to study the amplitude modulation for travelling waves when $\omega^2 > 0$, we now proceed to the second order problem in $O(\tilde{\varepsilon}^2)$. With the use of the first order solutions given by (9)–(13) on the right-hand sides of the second order equations, and solving the resulting equations, the second order solutions η_2, $\phi_2^{(j)}$ and $\psi_2^{(j)}$ $(j = 1, 2)$, take the form

$$\eta_2 = \left[\frac{(a'+\sigma_1)}{k}\frac{\partial A}{\partial x_1} + \frac{\sigma_1}{\omega}\frac{\partial A}{\partial t_1}\right] e^{i\theta} + \Lambda A^2 e^{2i\theta} + c.c. + \xi_2\,, \tag{16}$$

$$\phi_2^{(1)} = -\frac{i\omega(ky+a')\sinh(ky+a')}{k^2\cosh a'}\frac{\partial A}{\partial x_1}e^{i\theta} - \frac{i\omega(1+\sigma_1^2)}{2k\sigma_1}(\Lambda + k\sigma_1)\frac{\cosh 2(ky+a')}{\cosh 2a'}\ A^2 e^{2i\theta} + c.c. + B_2^{(1)}, \tag{17}$$

$$\begin{aligned}\phi_2^{(2)} = {} & \frac{i\omega\sigma_1}{k^2\sigma_2}\left[\frac{(ky-b')\sinh(ky-b')}{\cosh b'} + \left(\frac{a'}{\sigma_1} - \frac{a'}{\sigma_2}\right)\frac{\cosh(ky-b')}{\cosh b'}\right]\frac{\partial A}{\partial x_1}e^{i\theta} \\ & + \frac{i\omega(1+\sigma_2^2)}{2k\sigma_2}\left(\Lambda - \frac{k\sigma_1^2}{\sigma_2}\right)\frac{\cosh 2(ky-b')}{\cosh 2b'}A^2 e^{2i\theta} + c.c. + B_2^{(2)},\end{aligned} \tag{18}$$

$$\begin{aligned}\psi_2^{(1)} = {} & E_0^{(1)}\left[\left\{\frac{\sinh(ky+a') + (ky+a')\cosh(ky+a')}{k\cosh a'}\right\}\frac{\partial A}{\partial x_1} + \frac{\sinh(ky+a')}{\omega\cosh a'}\frac{\partial A}{\partial t_1}\right]e^{i\theta} \\ & + \frac{E_0^{(1)}(1+\sigma_1^2)}{2\sigma_1}(\Lambda + k\sigma_1)\frac{\sinh 2(ky+a')}{\cosh 2a'}\ A^2 e^{2i\theta} + c.c.,\end{aligned} \tag{19}$$

$$\psi_2^{(2)} = -\frac{E_0^{(2)}\sigma_1}{\sigma_2}\left[\left\{\left(\frac{a'}{\sigma_1}-\frac{b'}{\sigma_2}+1\right)\frac{\sinh(ky-b')}{k\cosh b'}+\frac{(ky-b')\cosh(ky-b')}{k\cosh b'}\right\}\frac{\partial A}{\partial x_1}+\frac{\sinh(ky-b')}{\omega\cosh b'}\frac{\partial A}{\partial t_1}\right]e^{i\theta}$$
$$-\frac{E_0^{(2)}(1+\sigma_2^2)}{2\sigma_2}\left(\Lambda-\frac{k\sigma_1^2}{\sigma_2}\right)\frac{\sinh 2(ky-b')}{\cosh 2b'}A^2e^{2i\theta}+c.c., \tag{20}$$

where ξ_2 (which represents the induced mean motion or the zero frequency correction to slow modulation of the fundamental mode), and $B_2^{(j)}$ are real functions of the slow scales x_1, x_2, t_1, and t_2 to be determined by considering the equations of higher orders, and

$$\Lambda = \frac{1}{G_1}\left[\frac{1}{2}\omega^2\sigma_1^2(1-\rho)-\frac{3\omega^2}{2}\left(1-\frac{\rho\sigma_1^2}{\sigma_2^2}\right)\right. \tag{21}$$
$$\left.+\frac{k^2\sigma_1^2}{2}\left\{\frac{V_2^2}{\sigma_2^2}(3-\sigma_2^2)-\frac{V_1^2}{\sigma_1^2}(3-\sigma_1^2\right\}\right],$$

where

$$G_1 = \frac{\omega^2}{k}(\sigma_1+\rho\sigma_2)-3k^2+k\left\{V_2^2\sigma_2+V_1^2\sigma_1\right\} \tag{22}$$

On substitution from (16)–(20) into the last condition of the second order equations, we obtain the non-secularity condition, which consists of two parts; one is

$$\frac{\partial A}{\partial t_1}+v_g\frac{\partial A}{\partial x_1}=0 \tag{23}$$

together with its c.c., where v_g (= dω/dk) is the group velocity of the wave train, and the other one is

$$(1-\rho)\xi_2+\frac{\partial B_1^{(1)}}{\partial t_1}-\rho\frac{\partial B_1^{(2)}}{\partial t_1}+G_2|A|^2=0, \tag{24}$$

where

$$G_2 = \sigma_1^2\left[\omega^2\left(\frac{1}{S_1^2}-\frac{\rho}{S_2^2}\right)-k^2\left(\frac{V_2^2}{S_2^2}-\frac{V_1^2}{S_1^2}\right)\right]$$

and

$$S_j^2 = \sigma_j^2/(1-\sigma_j^2), \quad j=1,2.$$

Equation (23) implies that, to the lowest order in $\tilde{\varepsilon}$, the complex amplitude A remains constant in a frame of reference moving with the group velocity v_g of the waves, that is, A depends on x_1 and t_1 only through ζ defined as $\zeta = x_1 - v_g t_1 = \tilde{\varepsilon}(x - v_g t)$. In (21), the case when $G_1 = 0$, for which η_2, $\phi_2^{(j)}$ and $\psi_2^{(j)}$ become infinite, corresponds to the case of second harmonic resonance which can be dealt with along the lines outlined by Singla et al. [20], in another problem of interest. Such a kind of resonance in our case will be discussed separately in another paper in the near future. In this section, we have assumed that this quantity is different from zero in (16)–(20).

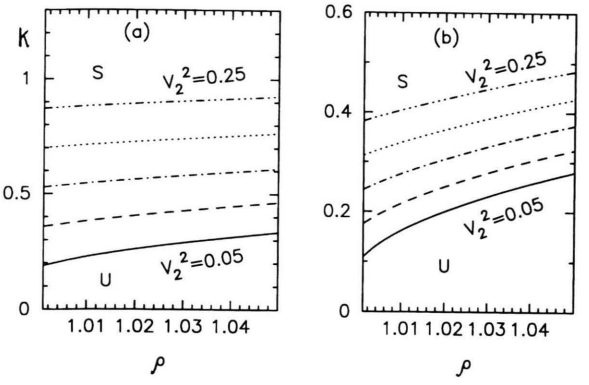

Fig. 2. Stability diagram for the system considered in Fig. 1b, but with (a) $a' = 0.9$, $b' = 0.3$, and (b) $a' = 0.3$, $b' = 0.9$.

5. Third Order Solution

Let us proceed to the third order problem. Introducing (9)–(13) and (16)–(20) into the third order perturbation equations and solving the resulting equations, we obtain the third order solutions η_3, $\phi_3^{(j)}$ and $\psi_3^{(j)}$ as indicated in the Appendix. On substitution from (A.1)–(A.5) into the last condition of the third order problem, we obtain the non-secularity condition from the coefficient of $e^{i\theta}$, that is

$$\frac{2\omega}{k}\left(1+\frac{\rho\sigma_1}{\sigma_2}\right)\left\{\frac{\partial A}{\partial t_2}+v_g\frac{\partial A}{\partial x_2}\right\}-\frac{i}{k}\left(1+\frac{\rho\sigma_1}{\sigma_2}\right)\frac{\partial^2 A}{\partial t_1^2}-\frac{2i\sigma_1}{k}\left\{\frac{v_g}{\sigma_1}\left(1+\frac{\rho\sigma_1}{\sigma_2}\right)+\omega\left(a\left(1+\frac{\rho}{\sigma_1\sigma_2}\right)-\frac{\rho b}{S_2^2}\right)\right\}$$
$$\cdot\frac{\partial^2 A}{\partial x_1\partial t_1}+\frac{i}{k}\left[\frac{\omega^2}{k^2}\left\{\frac{1}{4}\left(1+\frac{\rho\sigma_1}{\sigma_2}\right)-\frac{\rho b'\sigma_1}{S_2^2}\left(\frac{a'}{\sigma_1}-\frac{b'}{\sigma_2}\right)\right\}-\frac{1}{k}\left\{a'(1-\rho+3k^2)+\frac{\sigma_1}{4}(1-\rho+13k^2)\right\}\right.$$
$$\left.+\frac{V_2^2\sigma_1}{\sigma_2}\left(\frac{a'}{\sigma_1}-\frac{b'}{\sigma_2}\right)\left(2-\frac{b'\sigma_2}{S_2^2}\right)+2\sigma_1(V_2^2b'+V_1^2a')+\frac{4}{5}\left(\frac{V_2^2\sigma_1}{\sigma_2}+V_1^2\right)\right]\frac{\partial^2 A}{\partial x_1^2} \tag{25}$$
$$+iG_3A^2\bar{A}+i\left[\frac{G_2}{\sigma_1}\xi_2+2\omega\left(\frac{\partial B_1^{(1)}}{\partial x_1}+\frac{\rho\sigma_1}{\sigma_2}\frac{\partial B_1^{(2)}}{\partial x_1}\right)\right]A=0,$$

where

$$G_3=\omega^2\left\{\Lambda\left(\frac{\rho(\sigma_1+\sigma_2)(2+\sigma_1\sigma_2)}{\sigma_2^2}+\frac{\rho\sigma_1(1-2\sigma_2^2)}{\sigma_2^2}-\frac{(1-2\sigma_1^2)}{\sigma_1}\right)\right.$$
$$\left.+k\sigma_1\left(\frac{\rho(\sigma_2^2-\sigma_1^2)}{\sigma_2^3}-\frac{\rho\sigma_1^2(2-7\sigma_2^2)}{2\sigma_2^3}-\frac{(2-7\sigma_1^2)}{2\sigma_1}\right)\right\}$$
$$-k(1+\rho+k^2)\left\{(2+\sigma_1^2)\Lambda+\frac{k\sigma_1}{2}(2-\sigma_1^2)\right\}-\frac{3}{2}k^4\sigma_1^3+\frac{k^2V_2^2\sigma_1}{\sigma_2}$$
$$\cdot\left\{\left(\frac{(2+\sigma_1^2)}{\sigma_1}+\frac{(3-\sigma_2^2)}{\sigma_2}\right)\Lambda+\frac{k\sigma_1}{2}\left(\frac{(2-\sigma_1^2)}{\sigma_1}-\frac{4\sigma_1(1-2\sigma_2^2)}{\sigma_2^2}\right)\right\}$$
$$-k^2V_1^2\left\{\frac{(1-2\sigma_1^2)}{\sigma_1}\Lambda+\frac{k}{2}(2-7\sigma_1^2)\right\}.$$

Furthermore, from the non-secularity condition for η_3, we have

$$\frac{\partial\xi_2}{\partial t_1}+\frac{(a',-b')}{k}\frac{\partial B_1^{(j)}}{\partial x_1^2}+2\omega\sigma_1\left(1,-\frac{\sigma_1}{\sigma_2}\right)\frac{\partial|A|^2}{\partial x_1}=0. \tag{26}$$

If we assume that ξ_2, $B_1^{(j)}$ as well as A depend on x_1 and t_1 only through $\zeta=x_1-v_gt_1$, (26) yields

$$\left\{a'b'(1-\rho)-kv_g^2(b'+\rho a')\right\}\frac{\partial B_1^{(j)}}{\delta\zeta}= \tag{27}$$
$$k\left\{\frac{2\omega k\rho\sigma_1(\sigma_1+\sigma_2)}{\sigma_2}v_g^2(\rho,1)-2\omega\sigma_1(1-\rho)(b',-a'\sigma_1/\sigma_2)+v_g(-b',a')G_2\right\}|A|^2+f_j(x_2,t_2),$$

where we assume $v_g^2\neq ab(1-\rho)/(b+\rho a)$. The slow functions $f_j(x_2, t_2)$ in (27) are to be determined under appropriate boundary and/or initial conditions of the problem under consideration. Hereafter, however, we omit these terms, since they can be eliminated from the final result by a simple transformation [38] and cause no effect on the stability characteristics. Then ξ_2, $\partial B_1^{(j)}/\partial x_1$ in (25) can be expressed in terms of A. Using (23) and (24), introducing the expressions for ξ_2, $\partial B_1^{(j)}/\partial x_1$ into (25), and assuming that A depends on x_2 and t_2 through $\zeta_2=x_2-v_gt_2$ and $\tau=t_2$, we obtain finally a nonlinear Schrödinger equation

$$i\frac{\partial A}{\partial\tau}+\mu\frac{\partial^2 A}{\partial\zeta^2}+\nu|A|^2A=0, \tag{28}$$

where

$$\mu=\frac{1}{2}\frac{dv_g}{dk} \tag{29}$$

and

$$v=\frac{k}{2\omega}\left(1+\frac{\rho\sigma_1}{\sigma_2}\right)^{-1}\left[G_3+\frac{4}{\left\{a'b'(1-\rho)-kv_g^2(b'+\rho a')\right\}}\right. \tag{30}$$
$$\left.\cdot\left\{\frac{k^2\omega^2\rho\sigma_1(\sigma_1+\sigma_2)^2}{\sigma_2^2}v_g^2-\frac{k\omega^2\sigma_1(1-\rho)}{\sigma_2^2}(\rho a'\sigma_1^2+b'\sigma_2^2)+\frac{k\omega}{\sigma_2}v_g(\rho a'\sigma_1-b'\sigma_2)G_2-\frac{a'b'}{4\sigma_1}G_2^2\right\}\right],$$

where v is the nonlinear intercation coefficient; it should be noted that this coefficient becomes infinite and the perturbation scheme becomes invalid for values of k, ρ, $\varepsilon^{(j)}$, $E_0^{(j)}$, a and b which satisfy $v_g^2-ab(1-\rho)/(b+\rho a)=0$, which indicates that the group velocity of the wave train (i.e. v_g) coincides with the phase velocity of the infinitely long waves (i.e. $\sqrt{ab(1-\rho)/(b+\rho a)}$). In this case we have to modify the perturbation expansion so as to avoid the trouble of undboundedness. It is interesting to note that this case is expected to indicate a kind of resonant interaction between the group and phase velocities (i.e. between the short and the long waves); such a modification may be possible following the same lines as in [39].

6. Numerical Discussion

Equation (28) describes the nonlinear self-modulation of the capillary-gravity waves on liquid layers of uniform depths. It is interesting to note that the two coefficients μ and v are responsible for the modulational instability of a nonlinear plane wave solution of (28). The original wave train is stable or unstable if μv is positive or negative [5]. The nonlinear Schrödinger equation is well known to admit various types of envelope solitons according to the sign of μv.

(a) In the case of $\mu v > 0$

$$A_B(\zeta,\tau)=$$
$$A_0\operatorname{sech}(K_+\zeta)\exp\left\{i(vA_0^2/2)\tau\right\} \tag{31}$$

with

$$K_+=\sqrt{vA_0^2/2\mu}.$$

This convex envelope wave is called a bright soliton.

b) In the case of $\mu v < 0$

$$|A_D(\zeta,\tau)|^2=A_\infty^2-A_0^2\operatorname{sech}^2(K_-\zeta) \tag{32}$$

with

$$K_-=\sqrt{-vA_0^2/2\mu},\quad A_\infty > A_0 > 0.$$

This concave envelope wave is called a dark soliton or envelope hole. In this case, a shock type solution called a phase jump also exists:

$$A_P(\zeta,\tau)=A_0\tanh(K_-\zeta)\exp\left(i(A_0^2v)\tau\right). \tag{33}$$

The above envelope waves all stand steadily in (ζ, τ) space.

If in the nonlinear Schrödinger equation (28), we take the limit when $ka\to-\infty$ and $kb\to\infty$ (i.e. σ_1, $\sigma_2\to 1$), we recover the results obtained earlier by Mohamed and Elshehawey [29]. The results of Qi-su [7] for the corresponding pure hydrodynamical case can be obtained by setting $E_0^{(j)}=0$ or $\varepsilon^{(1)}=\varepsilon^{(2)}$ in the nonlinear Schrödinger equation (28). We should also remark here that for ideal fluids, in the limit of no capillarity, (28) recovers the result for the gravity waves obtained earlier by Tanaka [8].

As we mentioned before, the original wave train is stable or unstable if $\mu v > 0$ or $\mu v < 0$. The stability characteristics change critically depending on the values of $E_0^{(j)}$, $\varepsilon^{(j)}$, ρ, k, a, and b. The stability chart in the $k-\rho$ plane is divided into stable and unstable regions bounded by the curves.

$$\mu=0 \tag{34}$$

and

$$v=0. \tag{35}$$

We observe from (35) and (21) that v changes sign across the transition curves

$$G_1=0 \tag{36}$$

and

$$kv_g^2(b'+\rho a')-a'b'(1-\rho)=0, \tag{37}$$

which represent the third and fourth transition curves in the stability diagrams. We note from (29) and (30) that the stability of the system does note depend on which one of the fluids has a larger dielectric constant. We computed the relations (34)–(37) for different values of V_j^2 in the three cases $a'=b'$, $a'>b'$ and $a'<b'$, respectively, for values of the density ratio $\rho\le 1$. In the graphs, we plot the neutral stability conditions (34)–(37). Figures 3–9 represent the stability diagrams in the $k-\rho$

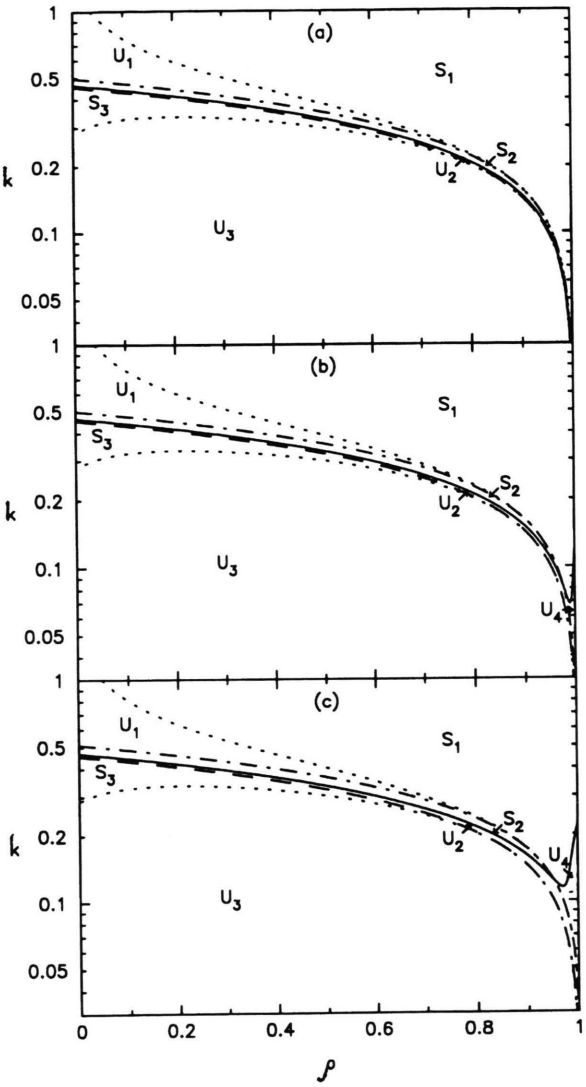

Fig. 3. Stability diagram for the nonlinearity effect in the k-ρ plane for $\rho \leq 1$ and $a' = b' = 0.9$. The solid, dotted, dashed and dot-dashed curves represent respectively equations (34)–(37), when (a) $V_1^2 = V_2^2 = 0$, (b) $V_1^2 = V_2^2 = 0.009$, and (c) $V_1^2 = 0.009$, $V_2^2 = 0.04$.

plane, due to the nonlinearity effect and the presence of the electric field, drawn for the three cases $a' = b'$, $a' > b'$ and $a' < b'$, respectively. Figures 3–5 represent the case $a' = b'$ (i.e. with two equal depths, wehre $a' = b' = 0.9$). In this case the resulting curves from (34)–(37) are represented by the solid, dotted, dashed and dot-dashed curves, respectively, and we notice that there are two dotted curves which correspond to (35), we refer to them as the upper and lower parts of the dotted curve.

In Fig. 3a, where $V_1^2 = V_2^2 = 0$ (the pure hydrodynamical case), there are three stable regions between the curves, the first region S_1 is above the upper part of the second curve, while the second stable region S_2 is between the first and the fourth curves, and the third region S_3 is between the third curve and the lower part of the second curve, respectively. There are three unstable regions too, the first region U_1 is between the upper part of the second curve and the fourth curve, the second unstable region U_2 is between the first and the third curves, and the third region U_3 is under the lower part of the second curve. In Figs. 3b, c, where $V_1^2 = 0.009$ and $V_2^2 = 0.009$. 0.04, respectively, we note that the solid curve goes up slightly, creating a new unstable region U_4 which increases due to increase the electric field values, and the regions S_1, S_3 decrease, while region S_2 increases; and the region U_1 decreases while the regions U_2 and U_3 increase. We note also that the upper part of the dotted curve and the fourth curve coincide at $\rho \geq 0.8$ and also the lower part of the dotted curve and the second curve.

In Figs. 4 we have $V_1^2 = 0.009$ and $V_2^2 = 0.08, 0.15$ and 0.3, respectively. The resulting curves here have the same behaviour as the curves in Fig. 3, but in addition we find that region U_4 increases and region S_2 in Fig. 4a is splite into two regions S_3 as in Figs. 4b, c, where the first region decreases and the second one increases due to the increase of the electric field values. A new stable region S_4 appears in Figure 4c.

In Fig. 5a, where $V_1^2 = 0.009$ and $V_2^2 = 0.5$, the curves still have the same behaviour as in Fig. 4, and we notice that the new stable region S_4 increases due to the increase of the electric field. In Figs. 5b, c, where $V_1^2 = 0.009$ and $V_2^2 = 0.8$, 1.0, respectively, we find that the solid curve drops and changes the situation mentioned in the previous figures where regions S_4, U_4 disappear and regions S_1 and S_2 increase. The first region of S_3 diminishes and the second region increases, and region U_2 changes its place. A new unstable region U_5 appears due to the increase of the electric field values. In Fig. 5c, we find that regions S_1, U_2, and U_5 increase, while regions U_1, U_3, and S_3 decrease, creating a new stable region S_5.

Figures 6 and 7 represent the case $a' > b'$ (i.e. when the lower depth is larger than the upper one, where $a' = 0.9$, $b' = 0.3$). In Fig. 6a where $V_1^2 = V_2^2 = 0$, we notice that we get curves quite similar to those in Fig. 3a for the case $a' = b'$, but in this case we have four stable regions and four unstable regions due to the intersection of the upper part of the second curve with the fourth curve (at $\rho \simeq 0.12$) producing two unstable regions U_1 instead of the first unstable region U_1 in the previous case, and

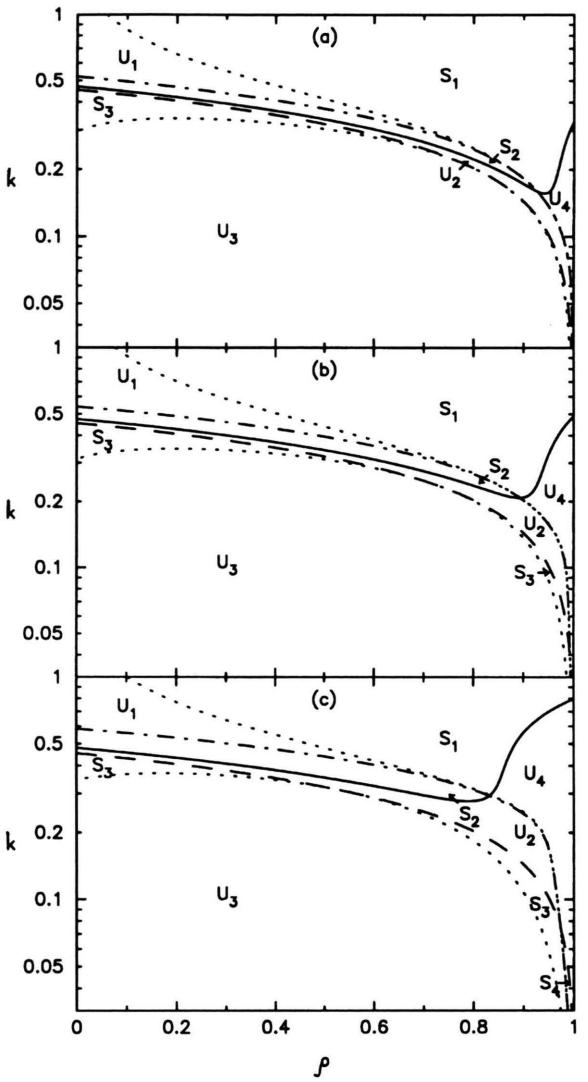

Fig. 4. Stability diagram for the system considered in Fig. 3, when $V_1^2 = 0.009$, but with (a) $V_2^2 = 0.08$, (b) $V_2^2 = 0.15$, and (c) $V_2^2 = 0.3$.

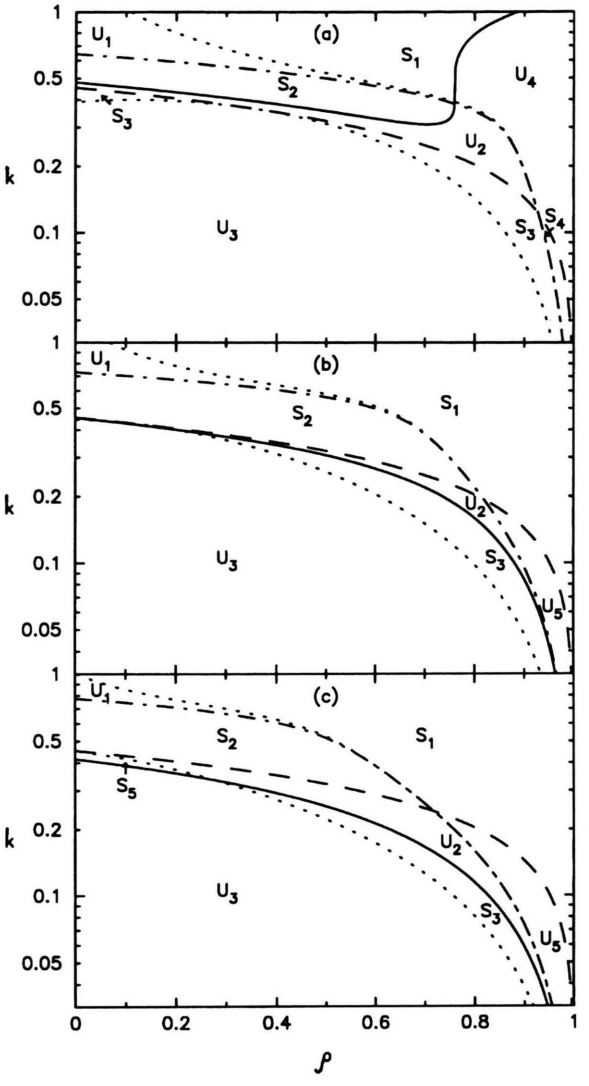

Fig. 5. Stability diagram for the system considered in Fig. 3, when $V_1^2 = 0.009$, but with (a) $V_2^2 = 0.5$, (b) $V_2^2 = 0.8$, and (c) $V_2^2 = 1$.

we call them the first and second parts of the first unstable region U_1. Also the intersection of the lower part of the second curve with the third curve (at $\rho \simeq 0.13$) produces two stable regions S_3 instead of the third stable region, and we call them too the first and second parts of the third stable region S_3.

In Figs. 6b, c, where $V_1^2 = 0.009$ and $V_2^2 = 0.005$ and 0.009, respectively, we notice that as in the previous case, the increase of the electric field slightly decreases the first stability region S_1 and the first part of the third region S_3, while it increases the second stability regon S_2 and the second part of the third region S_3. The two parts of the first unstable region U_1 decrease and the second unstable region U_2 increases while the third unstable region U_3 decreases. The solid curve turns out at $\rho \simeq 0.9$, creating a new unstable and stable regions U_4 and S_4, respectively, under it with further increasing of the electric field values as shown in Figures 7.

In Figures 7, where $V_1^2 = 0.009$ and V_2^2 =0.03, 0.055 and 0.08, respectively, we note that the behaviour of the

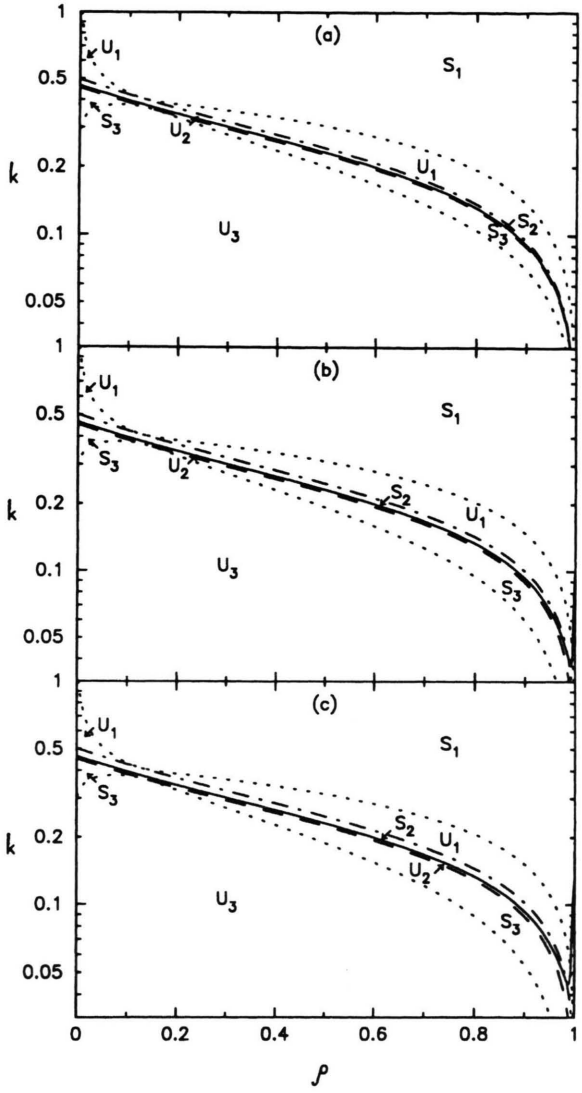

Fig. 6. Stability diagram for the nonlinearity effect in the k-ρ plane for $\rho \leq 1$ and $a' = 0.9, b' = 0.3$. The solid, dotted, dashed, and dot-dashed curves represent respectively equations (34)–(37), when (a) $V_1^2 = V_2^2 = 0$, (b) $V_1^2 = 0.009$, $V_2^2 = 0.005$, and (c) $V_1^2 = 0.009$, $V_2^2 = 0.009$.

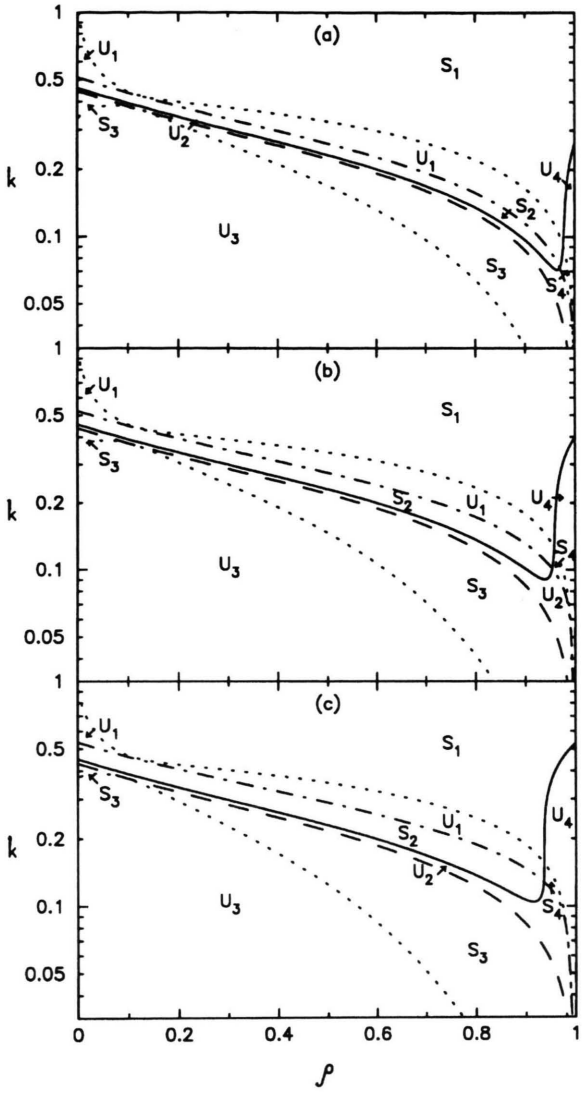

Fig. 7. Stability diagram for the system considered in Fig. 6, when $V_1^2 = 0.009$, but with (a) $V_2^2 = 0.03$, (b) $V_2^2 = 0.05$, and (c) $V_2^2 = 0.08$.

different curves and regions is still as before except that the solid curve goes up slightly, creating two new regions, one being unstable U_4 and the other one stable S_4 under it as in Figure 7a. It is clear from Figs. 7b, c that the increase of the electric field increases the new unstable region U_4 while it decreases the new stable region S_4; i.e. the normal electric field has a destabilizing effect in the two new regions.

Figures 8 and 9 represent the case $a' < b'$ (i.e. when the lower depth is smaller than the upper one, where $a' = 0.3, b' = 0.9$). Figure 8 are drawn for the electric field $V_1^2 = 0.009$ and $V_2^2 = 0.005$, 0.02 and 0.06, respectively. We notice that the curves have the same behaviour as in the case $a' = b'$ (i.e. we have three stable regions S_1, S_2, S_3 and three unstable regions U_1, U_2, U_3), and due to the increasing of the electric field as in Fig. 8b, the first and the third stability regions S_1 and S_3 decrease while the second stability region S_2 increases; and the three instability regions U_1, U_2 and U_3 increase. Also the solid curve goes up slightly, creating two new regions, one is

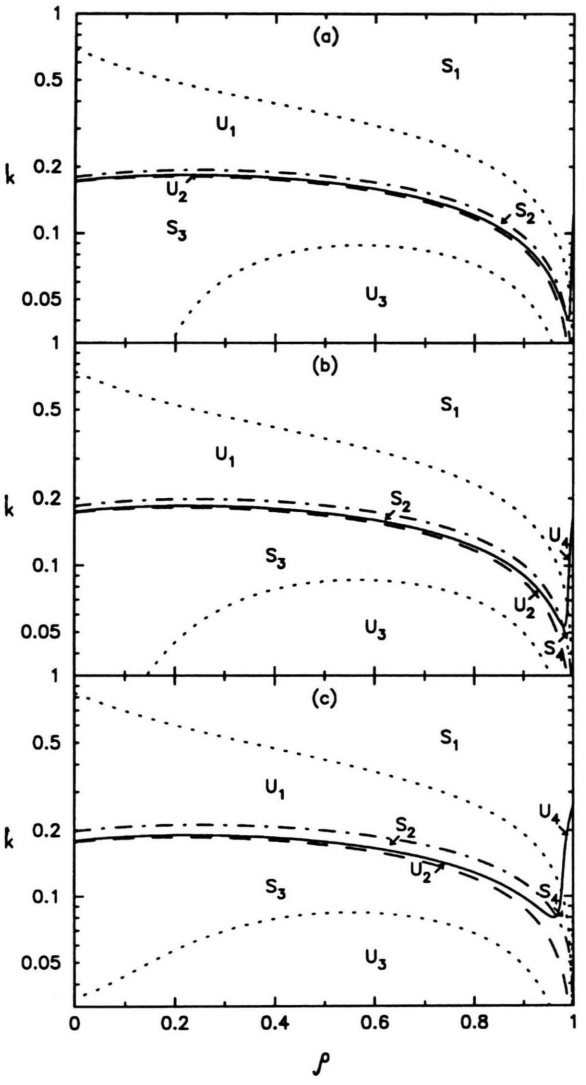

Fig. 8. Stability diagram for the nonlinearity effect in the k-ρ plane for $\rho \leq 1$ and $a' = 0.3$, $b' = 0.9$. The solid, dotted, dashed, and dot-dashed curves represent respectively equations (34)–(37), when $V_1^2 = 0.009$ and (a) $V_2^2 = 0.005$, (b) $V_2^2 = 0.02$, and (c) $V_2^2 = 0.06$.

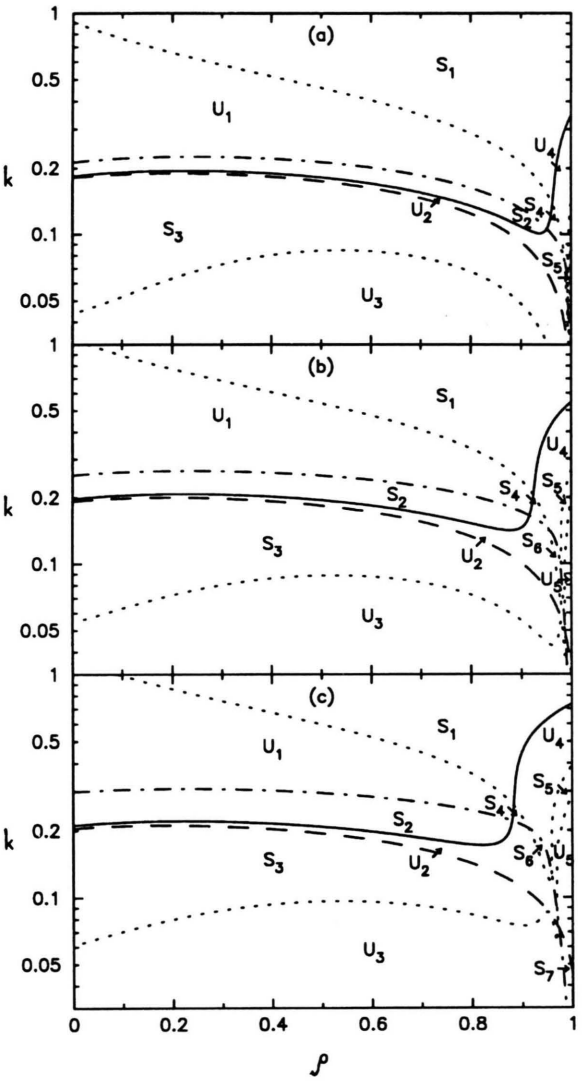

Fig. 9. Stability diagram for the system considered in Fig. 8, when $V_1^2 = 0.009$, but with (a) $V_2^2 = 0.1$, (b) $V_2^2 = 0.2$, and (c) $V_2^2 = 0.3$.

stable S_4 and the other one is unstable U_4 as shown in Figs. 8b, c in which the increase of the electric field increases region U_4 while decreases region S_4.

In Figs. 9, where $V_1^2 = 0.009$ and $V_2^2 = 0.1$, 0.2 and 0.3, respectively, we notice from Fig. 9a that the unstable region U_4 increases while the stable region S_4 decreases due to the increase of the electric field. Further values of the electric field produce a new stable regions S_5, S_6 and an unstable region U_5, as shown in Figure 9b. In Fig. 9c, we find that in addition to the previous behaviour of the curves, the three new regions S_5, S_6 and U_5 increase due to increasing the electric field, and also a new stable region S_7 appears.

Thus the effect of the electric field is the same in all the cases for small values of the electric field; and for a fixed value of V_1^2 and after a definite value of V_2^2, the effect of the electric field is different from one case to another, and it is stronger in the case when $a' > b'$.

7. Amplitude Modulation of Standing Waves

When k tends k_c, ω tends to zero, so that the group velocity v_g, and the coefficients μ and v given by (29) and (30), respectively, become infinite. Therefore the preceding obtained results are no longer valid near the cut-off wavenumber $k = k_c$, and we need to modify the preceding analysis to obtain the suitable equation for the complex amplitude near the cut-off wavenumber. Since we are concerned with waves near $k = k_c$ and $\omega = 0$, the carrier wave is not travelling, but standing, hence we choose the starting solutions to the first order problem as

$$\eta_1 = i\sigma_1 A e^{ik_c x_0} + c.c., \tag{38}$$

$$\phi_1^{(j)} = B_1^{(j)}, \quad j = 1,2, \tag{39}$$

$$\psi_1^{(1)} = iE_0^{(1)} \frac{\sinh(k_c y + a')}{\cosh a'} A e^{ik_c x_0} + c.c., \tag{40}$$

$$\psi_1^{(2)} = -\frac{iE_0^{(2)}\sigma_1}{\sigma_2} \frac{\sinh(k_c y - b')}{\cosh b'} \cdot A e^{ik_c x_0} + c.c. \tag{41}$$

instead of (9)–(13), where $a' = k_c a$ and $b' = k_c b$.

Proceeding as before, we can get the uniformly valid solution of the second order problem in the form

$$\eta_2 = \Lambda A^2 e^{2ik_c x_0} + c.c. + \xi_2, \tag{42}$$

$$\phi_2^{(1)} = \frac{i\cosh(k_c y + a')}{k_c \cosh a'} \frac{\partial A}{\partial t_1} e^{ik_c x_0} + c.c. + B_2^{(1)}, \tag{43}$$

$$\phi_2^{(2)} = -\frac{i\cosh(k_c y - b')}{k_c \cosh b'} \frac{\sigma_1}{\sigma_2} \frac{\partial A}{\partial t_1} e^{ik_c x_0} + c.c. + B_2^{(2)}, \tag{44}$$

$$\psi_2^{(1)} = \frac{E_0^{(1)}(1+\sigma_1^2)}{2\sigma_2}\left(\Lambda + k_c\sigma_1^2\right) \cdot \frac{\sinh 2(k_c y + a')}{\cosh 2a'} A^2 e^{2ik_c x_0} + c.c., \tag{45}$$

$$\psi_2^{(2)} = -\frac{E_0^{(2)}(1+\sigma_2^2)}{2\sigma_2}\left(\Lambda - \frac{k_c\sigma_1^2}{\sigma_2}\right) \cdot \frac{\sinh 2(k_c y - b')}{\cosh 2b'} A^2 e^{2ik_c x_0} + c.c., \tag{46}$$

where

$$\Lambda = \frac{k_c^2\sigma_1^2}{2}\left\{V_2^2\left(\frac{2}{\sigma_2^2} + \frac{1}{S_2^2}\right) - V_1^2\left(\frac{2}{\sigma_1^2} + \frac{1}{\sigma_1^2}\right)\right\} \cdot \left\{(V_2^2\sigma_2 + V_1^2\sigma_1) - 3k_c\right\}^{-1} \tag{47}$$

under the non-secular condition

$$\frac{\partial A}{\partial x_1} = 0, \tag{48}$$

which shows that the complex amplitude A is independent of the first slow scales x_1. This should be compared with (23) for the travelling waves.

Let us now proceed to the third order problem. After straightforward calculations, the requirement that the third order perturbation be non-secular yields

$$i\frac{\partial A}{\partial x_2} + \mu^* \frac{\partial^2 A}{\partial t_1^2} = v^* |A|^2 A + RA, \tag{49}$$

where

$$\mu^* = -\frac{1}{2}\frac{\partial^2 k}{\partial \omega^2}\bigg|_{\omega=0}, \tag{50}$$

$$v^* = -\frac{k_c}{2}\frac{\partial^2 k}{\partial \omega^2}\bigg|_{\omega=0}\left(\frac{1}{\sigma_1} + \frac{\rho}{\sigma_2}\right)^{-1} \cdot \left[\frac{3}{2}k_c^4\sigma_1^2 - k_c^2\Lambda\left\{V_2^2\left(\frac{2}{\sigma_2^2} + \frac{1}{S_2^2}\right) - V_1^2\left(\frac{2}{\sigma_1^2} + \frac{1}{S_1^2}\right)\right\} + 2k_c^3\sigma_1^2\left\{\frac{V_2^2}{\sigma_2}\left(\frac{1}{S_2^2} - 1\right) - \frac{V_1^2}{\sigma_1}\left(\frac{1}{S_1^2} - 1\right)\right\}\right], \tag{51}$$

and

$$R = -\frac{k_c^3}{2}\frac{\partial^2 k}{\partial \omega^2}\bigg|_{\omega=0}\left(\frac{1}{\sigma_1} + \frac{\rho}{\sigma_2}\right)^{-1} \cdot \left\{\frac{V_2^2}{S_2^2} - \frac{V_1^2}{S_1^2}\right\} E(x_2, t_2), \tag{52}$$

where $E(x_2, t_2)$ is a constant in the slow scales x_1 and t_1.

Equation (49) is also a nonlinear Schrödinger equation, with time and space variables interchanged and hence furnishes the amplitude modulation of standing waves. The linear interaction term RA in (49) causes on-

ly a phase shift and thus can be removed by using the transformation

$$A(x_2, t_1) = A \exp\left(-i \int^{x_2} R(x_2') \, dx_2' \right). \tag{53}$$

The nonlinear Schrödinger equation (49) now takes the form

$$i \frac{\partial A}{\partial x_2} + \mu^* \frac{\partial^2 A}{\partial t_1^2} = \nu^* |A|^2 A. \tag{54}$$

We now examine the plane wave solution of the form

$$A(x_2, t_1) = B_0 e^{i(Kx_2 - \Gamma t_1)} e^{-\int^{x_2} R(x_2') dx_2'}, \tag{55}$$

where B_0 is a complex constant, and K and Γ are real constants representing respectively the wavenumber and frequency shifts.

On substituting (55) into (54), we get the dispersion relation

$$\Gamma^2 = -\left(K + \nu^* |B_0|^2 \right) / \mu^*. \tag{56}$$

For Γ to become imaginary, we must have $K < \nu^* |B_0|^2$. Combining (55) with the carrier wave, we can determine the "nonlinear" cut-off wavenumber as

$$k_n = k_c \left[1 + \frac{\varepsilon |B_0|^2}{2} \frac{\partial^2 k}{\partial \omega^2} \bigg|_{\omega=0} \left(\frac{1}{\sigma_1} + \frac{\rho}{\sigma_2} \right)^{-1} \cdot \left[\frac{3}{2} k_c^4 \sigma_1^2 - k_c^2 \Lambda \left\{ V_2^2 \left(\frac{2}{\sigma_2^2} + \frac{1}{S_2^2} \right) - V_1^2 \left(\frac{2}{\sigma_1^2} + \frac{1}{S_1^2} \right) \right\} + 2 k_c^3 \sigma_1^2 \left\{ V_2^2 \left(\frac{1}{S_2^2} - 1 \right) - V_1^1 \left(\frac{1}{S_1^2} - 1 \right) \right\} \right] \right] - \frac{\varepsilon^2}{x_2} \int^{x_2} R(x_2') \, dx_2', \tag{57}$$

which shows that the nonlinear cut-off wavenumber k_n depends sensitively on the initial condition with respect to t_1. It is clear that the bandwidth of the spectrum is of $O(\tilde{\varepsilon})$ in the frequency space for the standing wave, i.e. it is of $O(\tilde{\varepsilon}^2)$ in the wavenumber space.

8. Conclusions

In this work, we have investigated the nonlinear electrohydrodynamic stability of interfacial capillary-gravity waves of two superposed dielectric fluids with uniform depths and solid walls under the influence of a normal electric field and in the presence of surface charges at the interface between the two fluids. In the linear electrohydrodynamic case, which is studied analytically elsewhere [25], we found (numerically) that the normal electric field has usually a destabilizing effect, and this effect is stronger when the depth of the lower fluid is greater than the depth of the upper one. The dielectric constant ratio does not play any significant role in the linear stability case studied here, in contrast with our previous result in the case when the surface charges on the interface are absent [36].

It is also found that the complex amplitude of quasi-monochromatic travelling waves can be described by a nonlinear Schrödinger equation in a frame of reference moving with the group velocity. The stability characteristics of a uniform wave train are examined both analytically and numerically on the basis of the nonlinear Schrödinger equation, and we found that the stability of the system does not depend on which of the fluids has a larger dielectric constant. We studied the three cases when the depth of the lower fluid is equal to or greater than or smaller than the depth of the upper fluid, respectively, in the case of presence (and absence) of the normal electric field force when there are surface charges at the interface. We found that the effect of the normal electric field is different for different regions or stability, depending on the values of the density ratio ρ, the wavenumber k, the depths of the two fluids a and b, and the electric field values V_1^2 and V_2^2.

In the first and the third cases, when $a' = b'$ and $a' < b'$, respectively, the stability diagrams when $V_1^2, V_2^2 = 0$ are divided by three stable regions and three unstable regions; and for small electric field values we found that the electric field has a destabilizing effect in the first and the third stability regions while it has a stabilizing influence in the second stable region. Two new regions ap-

pear, one of them is stable and the other is unstable, and they increase due to increase the electric field in the case $a' = b'$, while the new stable region decreases and the unstable region increased if $a' < b'$. For a fixed value of V_1^2 and after a definite value of V_2^2, the distribution of stable and unstable regions in the first case $a' = b'$ changes and two more stable and unstable regions appear and increase; while in the third case $a' < b'$, only two more stable and unstable regions appear and increase due to increase the electric field.

In the second case $a' > b'$, the stability diagram is divided by four stable and four unstable regions, and the effect of the electric field is destabilizing in the first stable and the first part of the third stable region, and stabilizing in the second stable and the second part of the third stable region. Two newly regions appear, one of them is unstable and the other one is stable, and the electric field increases the first new region and decreases the second new one.

Thus the effect of the electric field is the same in all the cases for small values of the electric field; and for a fixed value of V_1^2 and after a definite value of V_2^2, the effect of the electric field is different from one case to another, and it is stronger if $a' > b'$. Therefore the normal electric field, in the presence of surface charges at the interface, creates some new regions of stability and instability, which were hiden in the corresponding case when there are no charges at the interface between the two fluids [34].

We also recovered some previous work and limiting cases corresponding to, e.g. the pure hydrodynamical case, the case of two semi-infinite fluids, the case of capillary waves, etc.; and the results of the linear theory are confirmed. We treated our problem too in the case of standing waves near the cut-off wavenumber, which is governed also by a nonlinear Schrödinger equation with the roles of time and space are interchanged. We finally determined the nonlinear dispersion relation and the nonlinear effect on the cut-off wavenumber.

Appendix

The solutions of the third order problem are given by

$$\eta_3 = \left[-\frac{i(4a'+\sigma_1)}{4k^2}\frac{\partial^2 A}{\partial x_1^2} - \frac{i(a'+\sigma_1)}{k}\left\{\frac{1}{\omega}\frac{\partial^2 A}{\partial x_1 \partial t_1} + i\frac{\partial A}{\partial x_2}\right\} - \frac{i\sigma_1}{\omega}\left\{\frac{1}{\omega}\frac{\partial^2 A}{\partial t_1^2} + i\frac{\partial A}{\partial t_2}\right\} \right.$$
$$\left. -ik\left\{(2+\sigma_1^2)\Lambda + \frac{k\sigma_1}{2}(2-\sigma_1^2)\right\} A^2\bar{A} + ik\left\{\xi_2 + \frac{\sigma_1}{\omega}\frac{\partial B_1^{(1)}}{\partial x_1}\right\} A \right] e^{i\theta} + NSPT + c.c. + \xi_3, \tag{A.1}$$

$$\phi_3^{(1)} = -\frac{\omega}{k\cosh a'}\left[\left(\frac{y^2}{2} + ay + \frac{1}{4k^2}\right)\cosh(ky+a')\frac{\partial^2 A}{\partial x_1^2} + i(y+a)\sinh(ky+a')\frac{\partial A}{\partial x_2}\right] e^{i\theta}$$
$$+ NSPT + c.c. - \frac{1}{2}(y+a)^2\frac{\partial^2 B_1^{(1)}}{\partial x_1^2} + B_2^{(1)}, \tag{A.2}$$

$$\phi_3^{(2)} = \left[\frac{\omega}{k\cosh b'}\frac{\sigma_1}{\sigma_2}\left[\left\{\left(\frac{y^2}{2} - by + \frac{1}{4k^2}\right)\cosh(ky-b') + \frac{1}{k}\left(\frac{a'}{\sigma_1} - \frac{b'}{\sigma_2}\right)(y-b)\sinh(ky-b')\right\}\frac{\partial^2 A}{\partial x_1^2}\right.\right.$$
$$\left. + i(y-b)\sinh(ky-b')\frac{\partial A}{\partial x_2}\right] + \left[-\frac{\omega b\sigma_1}{k^2\sigma_2^2}\left(\frac{a'}{\sigma_1} - \frac{b'}{\sigma_2}\right)\frac{\partial^2 A}{\partial x_1^2} + \frac{i\omega\sigma_1}{k^2\sigma_2}\left(\frac{a'}{\sigma_1} - \frac{b'}{\sigma_2}\right)\frac{\partial A}{\partial x_2} + \frac{\omega(\sigma_1+\sigma_2)}{\sigma_2^2}\right.$$
$$\cdot\left\{(2+\sigma_1\sigma_2)\Lambda + \frac{k\sigma_1(\sigma_2-\sigma_1)}{\sigma_2}\right\} A^2\bar{A} - \left\{\frac{\omega(\sigma_1+\sigma_2)}{\sigma_2^2}\xi_2 + \frac{\sigma_1}{\sigma_2}\left(\frac{\partial B_1^{(1)}}{\partial x_1} - \frac{\partial B_1^{(2)}}{\partial x_1}\right)\right\} A \Bigg]$$
$$\left. \cdot \frac{\cosh(ky-b')}{\cosh b'}\right] e^{i\theta} + NSPT + c.c. - \frac{1}{2}(y-b)^2\frac{\partial^2 B_1^{(2)}}{\partial x_1^2} + B_3^{(2)}, \tag{A.3}$$

$$\psi_3^{(1)} = -iE_0^{(1)}\left[\frac{\sinh(ky+a')}{\cosh a'}\left[\frac{1}{k}\left\{\frac{1}{\omega}\frac{\partial^2 A}{\partial x_1\,\partial t_1}+i\frac{\partial A}{\partial x_2}\right\}+\frac{1}{\omega}\left\{\frac{1}{\omega}\frac{\partial^2 A}{\partial t_1^2}+i\frac{\partial A}{\partial t_2}\right\}-\frac{k}{\omega}\frac{\partial B_1^{(1)}}{\partial x_1}A\right]\right.$$
$$+\left[\left\{\frac{1}{k}\frac{\partial^2 A}{\partial x_1^2}+\frac{1}{\omega}\frac{\partial^2 A}{\partial x_1\,\partial t_1}+i\frac{\partial A}{\partial x_2}\right\}\frac{(y+a)\cosh(ky+a')}{\cosh a'}\right. \tag{A.4}$$
$$\left.\left.+\left(\frac{y^2}{2}+ay+\frac{1}{4k^2}\right)\frac{\sinh(ky+a')}{\cosh a'}\frac{\partial^2 A}{\partial x_1^2}\right]\right]e^{i\theta}+NSPT+c.c.,$$

$$\psi_3^{(2)} = \frac{iE_0^{(2)}\sigma_1}{\sigma_2}\left[\frac{\sinh(ky-b')}{\cosh b'}\left[\frac{(\sigma_2-b')}{k^2\sigma_2}\left(\frac{a'}{\sigma_1}-\frac{b'}{\sigma_2}\right)\frac{\partial^2 A}{\partial x_1^2}+\frac{1}{k}\left(\frac{a'}{\sigma_1}-\frac{b'}{\sigma_2}+1\right)\right.\right.$$
$$\cdot\left\{\frac{1}{\omega}\frac{\partial^2 A}{\partial x_1\partial t_1}+i\frac{\partial A}{\partial x_2}\right\}+\frac{1}{\omega}\left\{\frac{1}{\omega}\frac{\partial^2 A}{\partial t_1^2}+i\frac{\partial A}{\partial t_2}\right\}+k\left\{\left(\frac{(2+\sigma_1^2)}{\sigma_1}+\frac{(2+\sigma_2^2)}{\sigma_2}\right)\Lambda\right.$$
$$\left.\left.+\frac{k\sigma_1}{2}\left(\frac{(2-\sigma_1^2)}{\sigma_1}-\frac{\sigma_1(2-\sigma_2^2)}{\sigma_2^2}\right)\right\}A^2\overline{A}-k\left\{\frac{(\sigma_1+\sigma_2)}{\sigma_1\sigma_2}\xi_2+\frac{1}{\omega}\frac{\partial B_1^{(1)}}{\partial x_1}\right\}A\right] \tag{A.5}$$
$$+\left[\left\{\frac{1}{k}\left(\frac{a'}{\sigma_1}-\frac{b'}{\sigma_2}+1\right)\frac{\partial^2 A}{\partial x_1^2}+\frac{1}{\omega}\frac{\partial^2 A}{\partial x_1\partial t_1}+i\frac{\partial A}{\partial x_2}\right\}\frac{(y-b)\cosh(ky-b')}{\cosh b'}\right.$$
$$\left.\left.+\left(\frac{y^2}{2}-by+\frac{1}{4k^2}\right)\frac{\sinh(ky-b')}{\cosh b'}\frac{\partial^2 A}{\partial x_1^2}\right]\right]e^{i\theta}+NSPT+c.c.,$$

where here and hereafter *NSPT* represents terms that do not produce secular terms, and ξ_3, $B_3^{(1)}$ and $B_3^{(2)}$ are real functions of the slow scales x_1, x_2, t_1 and t_2 to be determined by considering the equations of higher orders.

Acknowledgements

We would like to thank Prof. P. Joos (University of Antwerp, Belgium) for his critical reading of the manuscript, and his useful comments and discussion during early stages of this work.

[1] M. J. Lighthill, Proc. Roy, Soc. London A **299**, 28 (1967).
[2] G. B. Whitham, Proc. Roy. Soc. London A **299**, 6 (1967).
[3] H. C. Yuen and B. M. Lake, Phys. Fluids **18**, 956 (1975).
[4] V. H. Chu and C. C. Mei, J. Fluid Mech. **41**, 873 (1970); **47**, 373 (1971).
[5] H. Hasimoto and H. Ono, J. Phys. Soc. Japan **33**, 805 (1972).
[6] V. E. Zakharov, Sov. Phys. Tech. Phys. **9**, 190 (1968).
[7] Z. Qi-su, Appl. Math. Mech. **3**, 255 (1982).
[8] M. Tanaka, J. Phys. Soc. Japan **51**, 2016 (1982).
[9] R. K. Chhabra and H. K. Khosla, Indian J. Eng. Mater. Sci. **1**, 111 (1994).
[10] P. Christodulides and F. Dias, Phys. Fluids **7**, 3013 (1995).
[11] T. Collin, F. Dias, and J.-M. Ghidaglia, Eur. J. Mech. B/ Fluids **14**, 775 (1995); Contemporary Math. **200**, 47 (1996).
[12] M. Jones, Can. Appl. Math. Quart. **2**, 352 (1994); Int. J. Non-Linear Mech. **31**, 41 (1996).
[13] D. P. Dolai, Proc. Indian Nat. Sci. Acad. **62**, 137 (1996).
[14] Z. Qingpu, Acta Mech. Sinica **12**, 24 (1996).
[15] D.-S. Lee, J. Phys. II, Paris **7**, 1045 (1997).
[16] Y. Kato, M. Okamura, and M. Oikaea, J. Phys. Soc. Japan **66**, 2665, 2675 (1997).
[17] S. O. Shiryaeva, O. A. Grigor'ev, and A. I. Grigor'ev, Tech. Phys. Lett. **19**, 186 (1993); Tech. Phys. **41**, 869 (1996).
[18] O. A. Grigor'ev and S. O. Shiryaeva, Tech. Phys. **41**, 23 (1996).
[19] A. T. Perez, P. A. Vazquez, and A. Castellanos, IEEE Trans. Ind. Appl. **31**, 761 (1995).
[20] R. K. Singla, R. K. Chhabra, and S. K. Trehan, Indian J. Pure Appl. Math. **27**, 807 (1996); Z. Naturforsch A **51**, 10 (1996).
[21] A. Gonzalez and A. Castellanos, J. Electrostat. **40–41**, 55 (1997).
[22] D. Koulova-Nebova and P. Atten, J. Electrostat. **40–41**, 185 (1997).
[23] Lord Rayleigh, The Theory of Sound, Macmillan 1894.
[24] G. G. Stokes, in Mathematical and Physical Papers, University Press, Cambridge 1880, Vol. 1, p. 197.

[25] J. R. Melcher, Field coupled surface waves, MIT Press, Cambridge MA 1963.
[26] D. H. Michael, Quart. Appl. Math. **35**, 345 (1977).
[27] B. K. Shivamoggi, Quart. Appl. Math. **37**, 423 (1979).
[28] R. Kant, R. K. Jindia, and S. K. Malik, Quart. Appl. Math. **39**, 23 (1981).
[29] A. A. Mohamed and E. F. Elshehawey, Phys. Fluids **26**, 1724 (1983).
[30] E. F. Elshehawey, Czech. J. Phys. **40**, 727 (1990).
[31] A. A. Mohamed, E. F. Elshehawey, and M. F. El-Sayed, J. Colloid Interface Sci. **169**, 65 (1995); J. Computat. Applied Math. **60**, 331 (1995).
[32] D. K. Callebaut and M. F. El-Sayed, Astrophys. Space Sci. **222**, 237 (1994); Phys. Lett. A **232**, 126 (1997).
[33] M. F. El-Sayed, Physica Scripta **55**, 350 (1997); Can. J. Phys. **75**, 499 (1997); Z. Naturforsch A **53** (1998), in press.
[34] M. F. El-Sayed and D. K. Callebaut, Physica Scripta **57**, 161 (1998); J. Colloid Interface Sci. **199** (1998) (in press).
[35] D. A. Saville, Annu. Rev. Fluid Mech. **29**, 27 (1997).
[36] M. F. El-Sayed, Ph. D.Thesis, University of Antwerp, Belgium 1994.
[37] A. H. Nayfeh, Perturbation Methods, Wiley, New York 1973.
[38] T. Kawahara, J. Phys. Soc. Japan **35**, 1537 (1973).
[39] A. C. Newel, SIAM J. Appl. Math. **35**, 650 (1978).